

Simple and Rapid Endotoxin Recognition Using a Dipicolylamine-Modified Fluorescent Probe with Picomolar-Order Sensitivity

Hiroshi Kimoto, Yota Suzuki, Yu Ebisawa, Masamitsu Iiyama, Takeshi Hashimoto, and Takashi Hayashita*



Cite This: *ACS Omega* 2022, 7, 25891–25897



Read Online

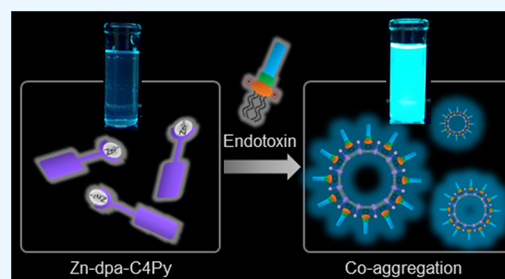
ACCESS |

Metrics & More

Article Recommendations

Supporting Information

ABSTRACT: Endotoxin is a lipopolysaccharide (LPS) that is found in the outer membrane of the cell wall of Gram-negative bacteria. Due to its high toxicity, the allowable endotoxin limit for water for injection is set at a very low value. Conventional methods for endotoxin detection are time-consuming and expensive and have low reproducibility. A previous study has shown that dipicolylamine (dpa)-modified pyrene-based probes exhibit fluorescence enhancement in response to LPS; however, the application of such probes to the sensing of LPS is not discussed. Against this backdrop, we have developed a simple and rapid endotoxin detection method using a dpa-modified pyrenyl probe having a zinc(II) center (Zn-dpa-C4Py). When LPS was added into Zn-dpa-C4Py solution, excimer emission of the pyrene moiety emerged at 470 nm. This probe can detect picomolar concentrations of LPS (limit of detection = 41 pM). The high sensitivity of the probe is ascribed to the electrostatic and hydrophobic interactions between the probe and LPS, which result in the dimer formation of the pyrene moieties. We also found that Zn-dpa-C4Py has the highest selectivity for LPS compared with other phosphate derivatives, which is probably caused by the co-aggregation of the probe with LPS. We propose that Zn-dpa-C4Py is a promising chemical sensor for the detection of endotoxin in medical and pharmaceutical applications.



1. INTRODUCTION

Endotoxin is a lipopolysaccharide (LPS) and the main component of the outer membrane of the cell wall of Gram-negative bacteria. LPS has an amphiphilic structure that is made up of three components: lipid A consisting of hydrophilic phosphorylated glucosamines and hydrophobic fatty acid chains, a core region, and a repeating unit (O-antigen) (Figure 1).^{1,2} This molecule is highly negatively

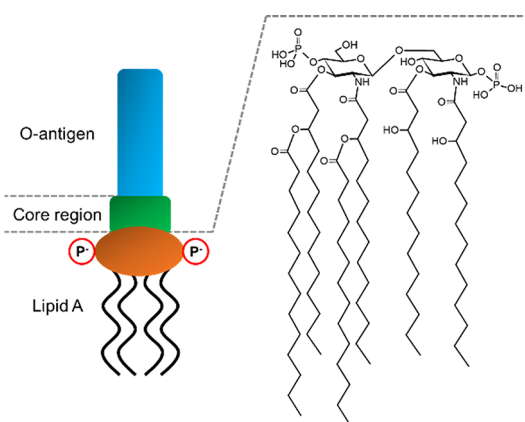


Figure 1. Schematic diagram of LPS (left) and structure of lipid A in *Escherichia coli* (right).

charged due to the phosphate groups and carboxyl groups.³ A tiny amount of endotoxin adversely affects the human immune system, causing fever, leukocytosis, tachycardia, and fatal multi-organ failure termed sepsis.^{4–6} In 2017, 11.0 million sepsis-related deaths were reported worldwide, which account for 19.7% of all global deaths.⁷ The European Pharmacopeia, the United States Pharmacopeia, and the Japanese Pharmacopeia have established a strict endotoxin limit of 0.25 EU/mL (EU = unit of measurement for endotoxin activity) for water for injection (WFI), which is highly purified, in order not to adversely affect a patient's safety.

Currently, endotoxin is detected either by the rabbit pyrogen assay, immune assays, and the limulus amoebocyte lysate (LAL) assay, which uses an aqueous extract of blood cells from the horseshoe crab, namely, LAL reagent or lysate reagent. The LAL assay is most widely used and has high sensitivity, thanks to a cascade system that amplifies the enzymatic reaction with endotoxin.⁸ On the other hand, this method requires a long measurement time,⁹ normally more than 60 min, and is

Received: June 14, 2022

Accepted: July 4, 2022

Published: July 15, 2022

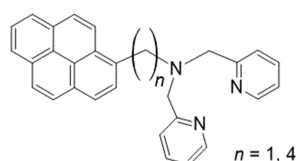


expensive.¹⁰ Moreover, there are unfavorable differences in reactivity among LAL reagent lots. Hence, an alternative technique to detect endotoxin is eagerly desired. Many attempts to establish new endotoxin detection methods have been made from various perspectives, e.g., electrochemistry, biochemistry, physical chemistry, and photochemistry, using aptamer, peptide, protein, graphene oxide, gold nanoparticle, quartz crystal unit, and fluorescent chemical sensors.^{11–13} In particular, fluorescent chemical sensors are appealing in terms of sensitivity, selectivity, and real-time detection.^{11,14} For example, Liu *et al.* designed and synthesized a series of pyridinium-functionalized dibenzo[*a,c*] phenazine fluorescent sensors for the selective detection of LPS and clarified the influence of the alkyl chain length in the probe molecule on their optical properties.³ Lim *et al.* reported peptide-assembled graphene oxide as a fluorescent Turn-ON chemical sensor for LPS, which has excellent sensitivity and the detection limit of 130 pM, one of the lowest values for a synthetic fluorescent chemical sensor to date.^{11,15} However, even this method is inferior to the LAL assay in terms of sensitivity. Moreover, many fluorescent chemical sensors for LPS require either time-consuming sample preparation or expensive materials.

We have reported several dipicolylamine (dpa)-modified fluorescent probes for the recognition of phosphate derivatives.^{16–19} The dpa moiety forms a chelate complex with a metal ion that has unoccupied coordination sites to which the oxygen atoms of the phosphate groups coordinate in water.¹⁹ The probes require neither cumbersome sample preparation nor costly substances. Thus, we expect that the dpa-modified probes will be able to detect LPS because LPS possesses several phosphate units in its structure. Meanwhile, Cabral *et al.* reported that the fluorescence intensity of several dpa-modified pyrene-based probes is enhanced by recognizing broad-spectrum bacteria, and for Gram-negative bacteria, they identified negatively charged membrane components including LPS as binding points between the probes and bacteria.²⁰ Moreover, they ascribed this fluorescence change to the excimer signal produced by the proximity-based stacking of multiple pyrene units through the chelated Zn²⁺ by dpa for phosphate binding. Although they were able to develop excellent chemical sensors, detailed experiments characterizing them as a practical LPS sensor were not fully carried out because their detection target was bacteria.

Herein, we report a simple and rapid detection method for LPS using the dpa-modified fluorescent probe reported by Cabral *et al.* (hereinafter denoted as dpa-C4Py). We synthesized two dpa-modified probes, dpa-C1Py and dpa-C4Py (Chart 1), to investigate the effect of the length of the spacer connecting the recognition site (dpa moiety) and the reporter site (pyrene moiety). The optical responses of these probes with various centered metal ions (M-dpa-C n Py, M = Co²⁺, Ni²⁺, Cu²⁺, Zn²⁺, and Cd²⁺) toward LPS were investigated by ultraviolet–visible (UV–vis) absorption and fluorescence measurements to determine the optimal sensor.

Chart 1. dpa-C n Py ($n = 1, 4$)



Particle size and zeta potential were also determined by dynamic light scattering (DLS) measurements to examine the morphology of the probe with LPS. Moreover, selectivity and interference assays were carried out using phosphate derivatives.

2. EXPERIMENTAL SECTION

Please refer to the Supporting Information for the reagents and the synthesis of dpa-C n Py (Schemes S1 and S2).

2.1. Apparatus. ¹H NMR spectra were measured using an Avance III HD 400 (Bruker Japan K. K., Kanagawa, Japan) at 400 MHz and JNM-ECA500 (JEOL Ltd., Tokyo, Japan) at 500 MHz at 298 K. All pH values were recorded using a Horiba F-52 pH meter (HORIBA, Ltd., Kyoto, Japan). UV–vis absorption spectra were measured using a 10 mm quartz cell and a Jasco V-760 UV–vis spectrophotometer (JASCO Corporation, Tokyo, Japan) equipped with a Peltier thermocontroller. Fluorescence spectra were measured using a 10 mm quartz cell and a HITACHI F-7000 fluorescence spectrophotometer (Hitachi High-Technologies, Co., Tokyo, Japan) equipped with a Peltier thermocontroller. DLS measurements were carried out at 25 °C using a Zetasizer Nano ZS (Malvern Instruments Ltd., Malvern, Worcestershire, UK).

2.2. Preparation of LPS stock solution. LPS from *Escherichia coli* O55: B5 (purified by phenol extraction) was dissolved in 5 mM HEPES buffer (pH 7.4). The LPS stock solution was vortexed for 3 min followed by sonication for 5 min.

2.3. Evaluation of the LPS Recognition Function of M-dpa-C n Py. The UV–vis and fluorescence spectra of dpa-C n Py with various metal ions were recorded in the absence and presence of 1.0 μM LPS. For titration tests, LPS was successively added into 10 μM M-dpa-C n Py solution until LPS concentration reached 1.0 μM. Each sample was measured within 1 min after the sample preparation. Fluorescence spectra were obtained at the excitation wavelength of 350 nm at 25 °C. The slit widths were set at 5 nm for both excitation and emission. The scan rate was set at 240 nm/min.

3. RESULTS AND DISCUSSION

3.1. LPS Recognition by M-dpa-C n Py. The LPS recognition functions of dpa-C1Py and dpa-C4Py were evaluated in the absence and presence of the following metal ions: Co²⁺, Ni²⁺, Cu²⁺, Zn²⁺, and Cd²⁺. In the absence of the metal ions, dpa-C4Py showed strong excimer emission centered at 470 nm (Figure S1). This is probably caused by the lower water solubility of dpa-C4Py, which possesses a longer alkyl chain, because such a result was not observed for dpa-C1Py. The excimer emission of dpa-C4Py was quenched by the addition of the metal ions except for Ni²⁺ (Figure 2 and Figure S1). The metal ions improved the solubility of the probes by complexation with the dpa moiety, which possibly brought about electrostatic repulsion among the probe molecules, leading to the monomerization of the pyrene dimers. On the other hand, we found that after the addition of 1 μM LPS into M-dpa-C4Py solution, the excimer emission of Zn-dpa-C4Py and Cd-dpa-C4Py was enhanced (Turn-ON), whereas that of the Ni²⁺ complex was diminished (Turn-OFF) (Figures 3 and 4). LPS seemingly coordinated to the centered metal ions of Zn²⁺ and Cd²⁺, resulting in the dimer formation of the pyrene moiety. The existence of intermolecular π–π

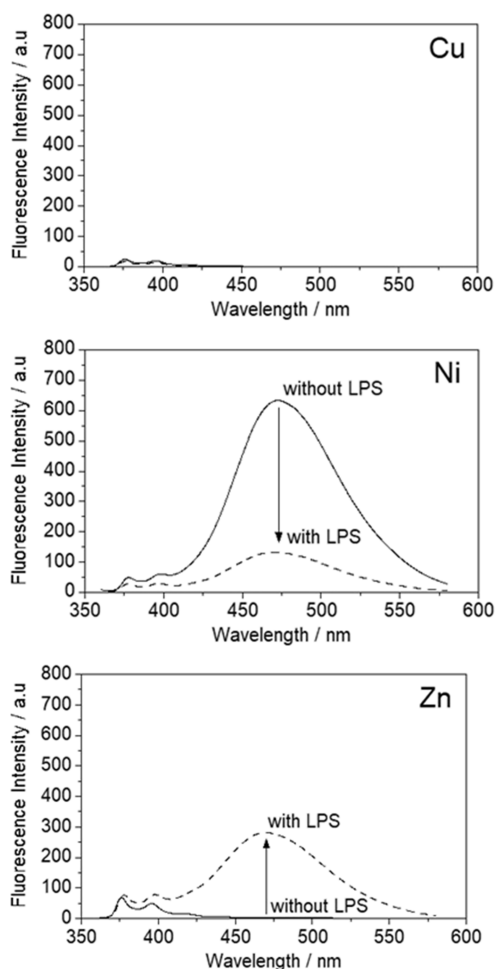


Figure 2. Fluorescence spectra of **M-dpa-C4Py** ($M = \text{Cu}^{2+}$, Ni^{2+} , and Zn^{2+}) without (solid line) and with (dashed line) $1 \mu\text{M}$ LPS in 1% DMSO/99% water (v/v) ($\lambda_{\text{ex}} = 350 \text{ nm}$). [**dpa-C4Py**] = 0.01 mM , [HEPES] = 5 mM , [$\text{M}(\text{NO}_3)_2$] = 0.01 mM , pH 7.4, and $25 \text{ }^\circ\text{C}$.

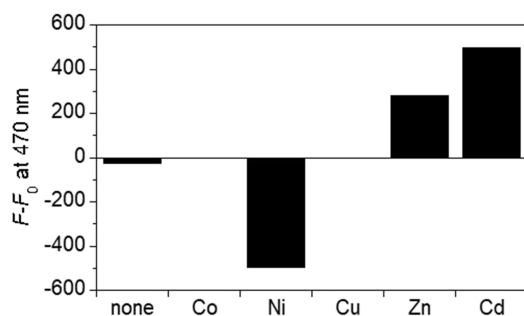


Figure 3. Changes in fluorescence intensity of **dpa-C4Py** and **M-dpa-C4Py** ($M = \text{Co}^{2+}$, Ni^{2+} , Cu^{2+} , Zn^{2+} , and Cd^{2+}) by the addition of $1 \mu\text{M}$ LPS in 1% DMSO/99% water (v/v) ($\lambda_{\text{ex}} = 350 \text{ nm}$). [**dpa-C4Py**] = 0.01 mM , [HEPES] = 5 mM , [$\text{M}(\text{NO}_3)_2$] = 0.01 mM , pH 7.4, and $25 \text{ }^\circ\text{C}$.

stacking of two pyrene moieties was also evidenced by the band broadening and the small redshifts in the UV–vis spectra (Figure S2).^{21,22} The removal of the metal ions from **dpa** by LPS, which can enhance excimer emission, did not occur because the UV–vis spectrum of **Zn-dpa-C4Py** with LPS was obviously different from that of **dpa-C4Py**; the absorption peaks of the probe clearly shifted to the shorter wavelength region by the addition of Zn^{2+} , and the absorbance was

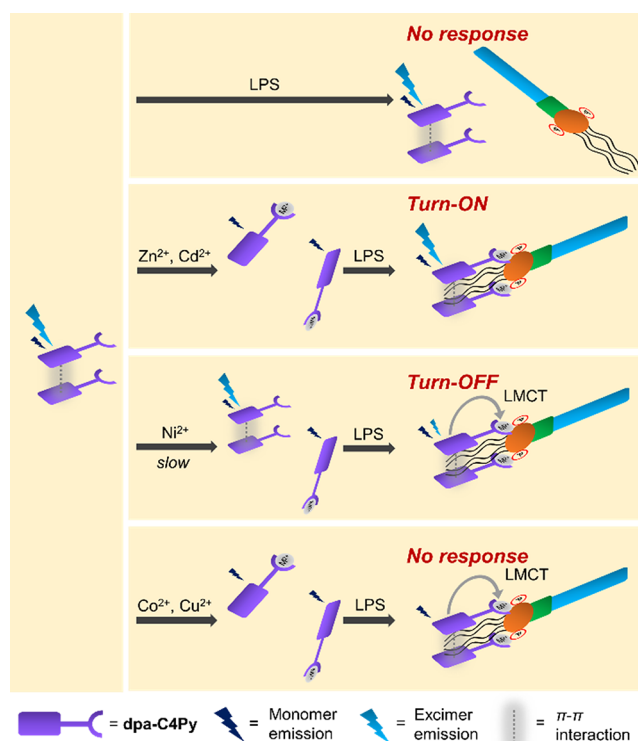


Figure 4. Proposed sensing mechanisms of **M-dpa-C4Py** ($M = \text{Co}^{2+}$, Ni^{2+} , Cu^{2+} , Zn^{2+} , and Cd^{2+}) for LPS.

decreased with a slight redshift by the addition of LPS (Figure S2). The Turn-OFF response toward LPS was unique to **Ni-dpa-C4Py** (Figure S3). The complexation rate of Ni^{2+} is known to be lower than those of the other divalent metals due to its electron configuration.²³ In fact, the intensity of the excimer emission decreased with time after the addition of Ni^{2+} into **dpa-C4Py** solution (Figure S4). Because Ni^{2+} was slowly coordinated by **dpa-C4Py**, the probe gradually dissolved with producing weak excimer emission (Figure 4). We found that the decrease rate of the excimer emission intensity was high when LPS co-existed (Figure S4). LPS may work as a surfactant to improve probe solubility in water. On the other hand, excimer emission was not enhanced by the addition of Co^{2+} and Cu^{2+} . Ligand-to-metal charge transfer (LMCT) plausibly occurs because Co^{2+} and Cu^{2+} possess unoccupied d-orbitals, whereas Zn^{2+} and Cd^{2+} are homologous elements of group 12 in the periodic table, and their d-orbitals are occupied by electrons (Figure 4).¹⁶

In contrast, little change in the fluorescence spectra of **dpa-C1Py** was observed by the addition of the metal ions and LPS (Figure S1). Hence, the length of the spacer drastically influenced the recognition abilities of the probes. The methylene spacer of **M-dpa-C1Py** would be too short or too rigid to form the pyrene dimer upon binding to LPS.

From the perspective of practical sensors, the Turn-ON response is generally preferable because it can be clearly distinguished from the background emission.²⁴ In addition, because Cd is highly toxic, we selected **Zn-dpa-C4Py** as the best candidate for practical usage, and the feasibility of this probe was further investigated, as described below.

3.2. Titration of LPS by Zn-dpa-C4Py. Figure 5 shows the fluorescence spectra of **Zn-dpa-C4Py** with different LPS concentrations. The excimer emission at 470 nm was dramatically enhanced by increasing the concentration of

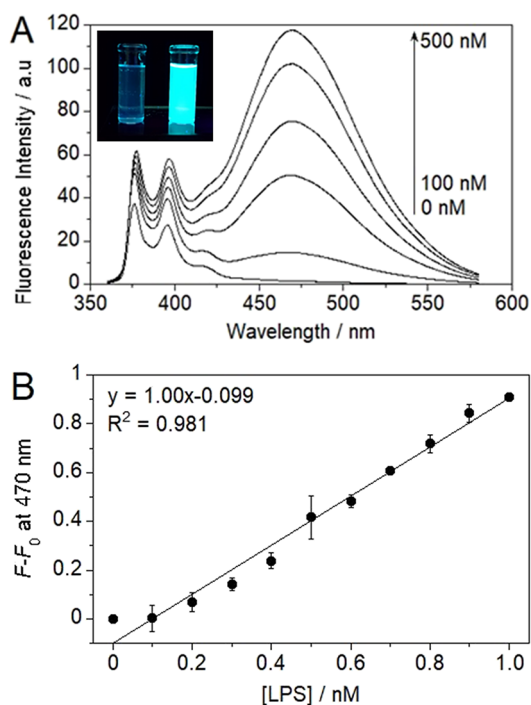


Figure 5. Fluorescence titration spectra of Zn-dpa-C4Py upon addition of LPS (A) and calibration curve (B) in 1% DMSO/99% water (v/v) ($\lambda_{\text{ex}} = 350$ nm). The inset in (A) is a photograph of the corresponding color change in the absence (left) and presence (right) of 1 μM LPS under UV irradiation in the dark. [dpa-C4Py] = 0.01 mM, [HEPES] = 5 mM, [Zn(NO₃)₂] = 0.01 mM, pH 7.4, and 25 °C. Each data point is the average of five measurements under the same conditions.

LPS. Furthermore, the change in emission color was clearly observed by the naked eye under UV irradiation in the presence of LPS (Figure 5A and Figure S5). The fluorescence intensity was increased linearly with increasing LPS from 0.1 to 1 nM. The limit of detection (LOD) was determined to be 41 pM. To the best of our knowledge, this LOD is the lowest among those of reported synthetic fluorescent chemical sensors for LPS (Table 1).

3.3. Sensing Mechanism. From the spectrum change obtained by the titration experiment, we calculated the Py value (Figure 6), which is the ratio of the fluorescence intensities of pyrene band I (375 nm)/band III (385 nm) at various LPS concentrations. This value describes the polarity of the microenvironment around the probe; a higher Py value indicates a more polar environment.^{38–40} Judging from Figure 6, the probe existed in a more hydrophobic environment with increasing concentration of LPS. It is likely that the probe self-assembles with LPS because LPS forms aggregates like micelles/vesicles in water (Figure 7).^{41–43} Amphiphilic Zn-dpa-C4Py possessing hydrophobic *n*-butyl pyrene and cationic Zn²⁺ coordinated by dpa will show high affinity toward the fatty acid chains and the phosphate groups of LPS. The decline of Py value caused by LPS addition was also reported using pyrene to investigate the aggregation behavior of LPS in the micromolar order.⁴¹ However, Zn-dpa-C4Py showed the decline of Py value at lower concentrations of LPS in the nanomolar order. The positive divalent charge of Zn²⁺ probably offsets the negative charge of the phosphate groups in LPS to facilitate the aggregation of LPS at lower concentration because the counter ions of ionic amphiphiles

Table 1. Comparison of Reported Synthetic Fluorescent Chemical Sensors for LPS with Zn-dpa-C4Py^a

fluorescent probe	LOD (pM)	reaction time (min)	ref
GO	130	N/A	15
QD-Apt-GO	870	30	26
ROX-LBA/GO	1570	N/A	27
MTA-Au	N/A	20	28
HDT-AuNPs	650	N/A	29
[Pt(NANAN)Cl] ⁺	5700	N/A	30
CPT1	270	N/A	31
peptide-diacetylene amphiphiles	N/A	N/A	32
BD2C	2600	N/A	3
TPEPyE	370	N/A	33
BT-5	120	0.5	34
CTPY-P16	6970	N/A	35
DMQA	100,000	N/A	22
BPTG	5000	N/A	36
Sp-Py	1000–10,000	N/A	37
Zn-dpa-C4Py	41*	<1	this work

^aThe molecular weight of LPS was assumed to be 10 kDa to calculate LOD in pM units.^{15,25} *41 pM is equivalent to 4.1 EU/mL, given that 100 pg/mL of LPS corresponds to 1 EU/mL.⁴³

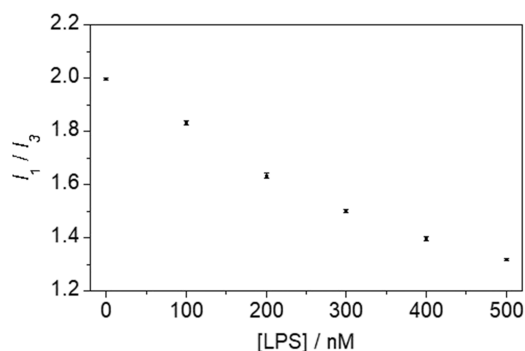


Figure 6. Py values of Zn-dpa-C4Py at various LPS concentrations shown in Figure 5. Each plot is the average of five measurements under the same conditions.

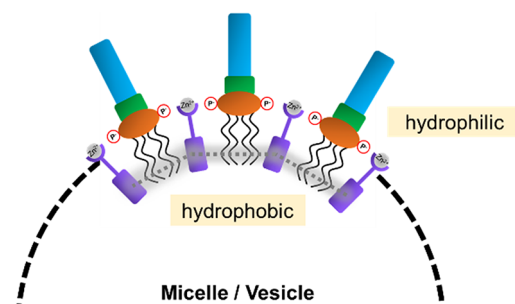


Figure 7. Schematic diagram of the co-aggregation of Zn-dpa-C4Py with LPS.

generally reduce the charge repulsion between the amphiphiles and lower the critical micelle concentration.

To elucidate the co-aggregation behavior, we measured the particle size distribution and the zeta potential by the DLS technique (Figure 8). The results showed that LPS itself formed particles measuring 39 ± 4 nm in diameter, which is consistent with reported data (10–50 nm range).^{41,44,45} The

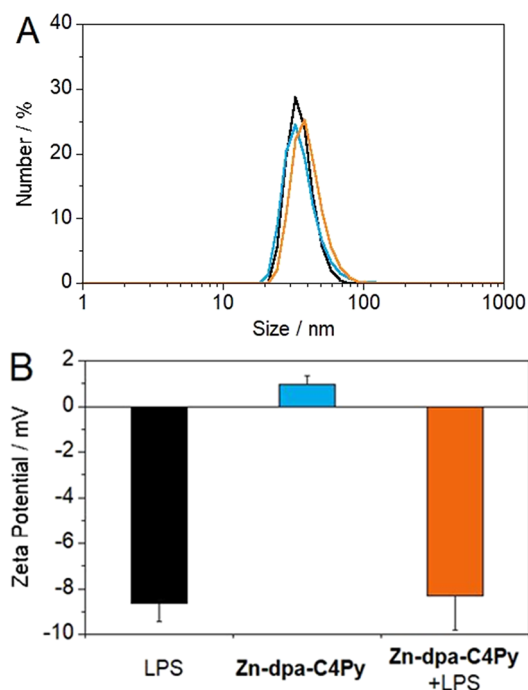


Figure 8. Size distribution (A) and zeta potential (B) of micelles/vesicles formed by LPS, Zn-dpa-C4Py, and the complex of Zn-dpa-C4Py with LPS, respectively, in 5 mM HEPES (pH 7.4). Each result is the average of three measurements under the same conditions.

average particle size of Zn-dpa-C4Py was 31 ± 13 and 36 ± 4 nm before and after the addition of LPS, respectively, suggesting that Zn-dpa-C4Py formed micelles/vesicles even without LPS because of its amphiphilic structure. Although the particle sizes were almost identical, each peak showed a near-Gaussian distribution, indicating that each compound formed almost homogeneous aggregates. The zeta potential of LPS particles was -8.6 ± 0.8 mV, which is consistent with reported values (-14 to -6 mV).^{45–47} This negative charge is derived from the phosphate groups and carboxyl groups. In contrast, Zn-dpa-C4Py showed the positive value of 1.0 ± 0.4 mV because of the charge of Zn^{2+} . We found that Zn-dpa-C4Py showed the zeta potential of -8.3 ± 1.5 mV in the presence of LPS, implying the formation of a supramolecular complex with LPS.

We conclude that surfactant-like Zn-dpa-C4Py recognized amphiphilic LPS through multiple points including negative phosphate groups and hydrophobic fatty acid chains by forming co-aggregates like micelles/vesicles. Then, the pyrene moieties of the sensor got close to each other, resulting in the excimer emission at 470 nm. It is possible that the aggregate formation enables sensitive detection for the following reasons: (1) it increases the local concentration of LPS from bulk water, and (2) it boosts the fluorescence response to LPS such as several sensors exploiting micelle formation with enhanced quantum yield.^{14,48,49}

3.4. Selectivity of Zn-dpa-C4Py. The selectivity of Zn-dpa-C4Py was evaluated by monitoring its fluorescence response to other biologically important phosphate derivatives (Pi: phosphate, PPI: pyrophosphate, Tri: triphosphate, AMP: adenosine monophosphate, ADP: adenosine diphosphate, and ATP: adenosine triphosphate) as possible interferents. Figure 9 shows that LPS displayed the strongest excimer fluorescence enhancement compared with the other phosphate interferents

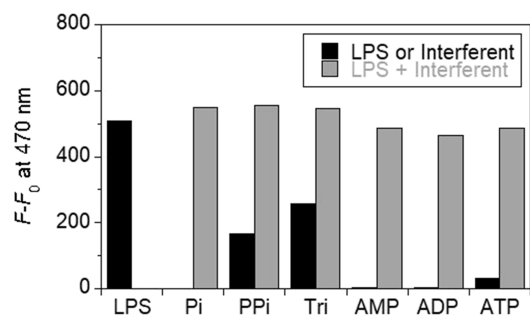


Figure 9. Changes in fluorescence intensity of Zn-dpa-C4Py in the presence of phosphate derivatives in 1% DMSO/99% water (*v/v*) ($\lambda_{\text{ex}} = 350$ nm). $[\text{dpa-C4Py}] = 0.01$ mM, $[\text{HEPES}] = 5$ mM, $[\text{Zn}(\text{NO}_3)_2] = 0.01$ mM, pH 7.4, and 25 °C.

(black columns). Cho *et al.* reported that Zn-dpa-C4Py is a pyrophosphate sensor but did not evaluate LPS as an analyte.⁵⁰ We demonstrated that this sensor recognized LPS more selectively than the other pyrophosphate derivatives. Moreover, small effects on LPS sensing by the other phosphate derivatives were found in the interference assay (gray columns). The large amount of negatively charged groups on the LPS molecules including two phosphate groups in lipid A make LPS highly negatively charged.⁴⁷ The difference in the number of phosphates per unit molecule and the highly negative charge of LPS probably contributed to the excellent selectivity of the probe for LPS because of the more recognition targets for dpa moieties and the strong electrostatic attraction between LPS and the positively charged sensor. A similar mechanism was reported for the positively charged tetraphenylethylene-based sensor for LPS.³³ In addition, the two-point sensing mechanism and the co-aggregation described above seemed to produce a stronger binding affinity and signal toward LPS.

4. CONCLUSIONS

Zn-dpa-C4Py showed pyrene-moiety-derived excimer emission after the addition of LPS without cumbersome sample preparation. Fluorescence measurements demonstrated that the probe formed co-aggregates with LPS by multi-point recognition of LPS through electrostatic and hydrophobic interactions, leading to the formation of pyrene dimers. Zn-dpa-C4Py showed excellent sensitivity down to the picomolar order (LOD = 41 pM), which is the best among the reported synthetic fluorescent chemical sensors for LPS. Furthermore, selectivity and interference assays using a series of phosphate derivatives revealed that the selectivity of this probe was the highest for LPS and interference was limited even in the presence of the other phosphate derivatives. This fluorescent Turn-ON sensor offers great potential for practical endotoxin/LPS detection to control the quality of pure water used in pharmaceuticals and dialysis.

■ ASSOCIATED CONTENT

Supporting Information

The Supporting Information is available free of charge at <https://pubs.acs.org/doi/10.1021/acsomega.2c02935>.

Reagents, (Scheme S1) synthesis of dpa-C1Py, (Scheme S2) synthesis of dpa-C4Py, (Figures S1–S5) LPS recognition by dpa-C*n*Py, and determination of LOD (PDF)

AUTHOR INFORMATION

Corresponding Author

Takashi Hayashita – Department of Materials and Life Sciences, Faculty of Science and Technology, Sophia University, Tokyo 102-8554, Japan; orcid.org/0000-0003-1264-9694; Email: ta-hayas@sophia.ac.jp

Authors

Hiroshi Kimoto – Department of Materials and Life Sciences, Faculty of Science and Technology, Sophia University, Tokyo 102-8554, Japan; Technical Development Division, Nomura Micro Science Co., Ltd., Atsugi, Kanagawa 243-0021, Japan; orcid.org/0000-0002-0803-6919

Yota Suzuki – Department of Materials and Life Sciences, Faculty of Science and Technology, Sophia University, Tokyo 102-8554, Japan; orcid.org/0000-0002-6182-8042

Yu Ebisawa – Department of Materials and Life Sciences, Faculty of Science and Technology, Sophia University, Tokyo 102-8554, Japan; Present Address: Idemitsu Kosan Co., Ltd., 1–1 Anesakikagan, Ichihara-shi, Chiba 299–0193, Japan

Masamitsu Iiyama – Technical Development Division, Nomura Micro Science Co., Ltd., Atsugi, Kanagawa 243-0021, Japan

Takeshi Hashimoto – Department of Materials and Life Sciences, Faculty of Science and Technology, Sophia University, Tokyo 102-8554, Japan

Complete contact information is available at:

<https://pubs.acs.org/10.1021/acsomega.2c02935>

Author Contributions

H.K., M.I., and T. Hayashita conceptualized the work. H.K., Y.S., M.I., T. Hashimoto, and T. Hayashita designed the experiments. H.K. and Y.E. conducted the experiments. All the authors were involved in the data analysis. H.K., Y.S., T. Hashimoto, and T. Hayashita wrote the manuscript. All the authors have given approval to the final version of the manuscript.

Notes

The authors declare no competing financial interest.

ACKNOWLEDGMENTS

This research was funded by a Grant-in-Aid for Scientific Research (C) (grant no. 18K05180) and a Grant-in-Aid for Scientific Research (B) (grant no. 20H02772) from the Japan Society for the Promotion of Science (JSPS). We are grateful to the members of the Analytical Chemistry Research Group of Sophia University for active discussions through this research.

REFERENCES

- (1) Barkleit, A.; Moll, H.; Bernhard, G. Interaction of uranium(VI) with lipopolysaccharide. *Dalton Trans.* **2008**, 2879–2886.
- (2) Imoto, M.; Kusumoto, S.; Shiba, T.; Rietschel, E. T.; Galanos, C.; Lüderitz, O. Chemical structure of *Escherichia coli* lipid A. *Tetrahedron Lett.* **1985**, *26*, 907–908.
- (3) Liu, X.; Yang, Z.; Xu, W.; Chu, Y.; Yang, J.; Yan, Y.; Hu, Y.; Wang, Y.; Hua, J. Fine tuning of pyridinium-functionalized dibenzo-*[a,c]*phenazine near-infrared AIE fluorescent biosensors for the detection of lipopolysaccharide, bacterial imaging and photodynamic antibacterial therapy. *J. Mater. Chem. C* **2019**, *7*, 12509–12517.
- (4) Wood, S. J.; Miller, K. A.; David, S. A. Anti-endotoxin agents. 1. Development of a fluorescent probe displacement method optimized

for high-throughput identification of lipopolysaccharide-binding agents. *Comb. Chem. High Throughput Screening* **2004**, *7*, 239–249.

(5) Pérez-Lorenzo, E.; Zuzuarregui, A.; Arana, S.; Mujika, M. Development of a biological protocol for endotoxin detection using quartz crystal microbalance (QCM). *Appl. Biochem. Biotechnol.* **2014**, *174*, 2492–2503.

(6) Hurley, J. C. Endotoxemia: methods of detection and clinical correlates. *Clin. Microbiol. Rev.* **1995**, *8*, 268–292.

(7) Rudd, K. E.; Johnson, S. C.; Agesa, K. M.; Shackelford, K. A.; Tsoi, D.; Kievlan, D. R.; Colombara, D. V.; Ikuta, K. S.; Kisson, N.; Finfer, S.; Fleischmann-Struzek, C.; Machado, F. R.; Reinhart, K. K.; Rowan, K.; Seymour, C. W.; Watson, R. S.; West, T. E.; Marinho, F.; Hay, S. I.; Lozano, R.; Lopez, A. D.; Angus, D. C.; Murray, C. J. L.; Naghavi, M. Global, regional, and national sepsis incidence and mortality, 1990–2017: analysis for the Global Burden of Disease Study. *Lancet.* **2020**, *395*, 200–211.

(8) Iwanaga, S. Biochemical principle of Limulus test for detecting bacterial endotoxins. *Proc. Jpn. Acad. Ser. B. Phys. Biol. Sci.* **2007**, *83*, 110–119.

(9) Ito, K.; Inoue, K. Y.; Ino, K.; Matsue, T.; Shiku, H. A highly sensitive endotoxin sensor based on redox cycling in a nanocavity. *Analyst* **2019**, *144*, 3659–3667.

(10) Sulc, R.; Szekeley, G.; Shinde, S.; Wierzbicka, C.; Vilela, F.; Bauer, D.; Sellergren, B. Phospholipid imprinted polymers as selective endotoxin scavengers. *Sci. Rep.* **2017**, *7*, 44299.

(11) Sondhi, P.; Maruf, M. H. U.; Stine, K. J. Nanomaterials for biosensing lipopolysaccharide. *Biosensors* **2019**, *10*, 2.

(12) Su, W.; Ding, X. Methods of endotoxin detection. *J. Lab. Autom.* **2015**, *20*, 354–364.

(13) Stromberg, L. R.; Mendez, H. M.; Mukundan, H. Detection methods for lipopolysaccharides: past and present. *IntechOpen* **2017**, 141–166.

(14) Ding, L.; Bai, Y.; Cao, Y.; Ren, G.; Blanchard, G. J.; Fang, Y. Micelle-induced versatile sensing behavior of bispyrene-based fluorescent molecular sensor for picric acid and PYX explosives. *Langmuir* **2014**, *30*, 7645–7653.

(15) Lim, S. K.; Chen, P.; Lee, F. L.; Mochhala, S.; Liedberg, B. Peptide-assembled graphene oxide as a fluorescent turn-on sensor for lipopolysaccharide (endotoxin) detection. *Anal. Chem.* **2015**, *87*, 9408–9412.

(16) Yamada, T.; Fujiwara, S.; Fujita, K.; Tsuchido, Y.; Hashimoto, T.; Hayashita, T. Development of dipicolylamine-modified cyclodextrins for the design of selective guest-responsive receptors for ATP. *Molecules* **2018**, *23*, 635.

(17) Fujita, K.; Fujiwara, S.; Yamada, T.; Tsuchido, Y.; Hashimoto, T.; Hayashita, T. Design and function of supramolecular recognition systems based on guest-targeting probe-modified cyclodextrin receptors for ATP. *J. Org. Chem.* **2017**, *82*, 976–981.

(18) Aoki, K.; Osako, R.; Deng, J.; Hayashita, T.; Hashimoto, T.; Suzuki, Y. Phosphate-sensing with (di-(2-picolyl)amino) quinazolines based on a fluorescence on–off system. *RSC Adv.* **2020**, *10*, 15299–15306.

(19) Tsuchido, Y.; Yamasawa, A.; Hashimoto, T.; Hayashita, T. Metal and phosphate ion recognition using dipicolylamine-modified fluorescent silica nanoparticles. *Anal. Sci.* **2018**, *34*, 1125–1130.

(20) Cabral, A. D.; Rafiei, N.; de Araujo, E. D.; Radu, T. B.; Toutah, K.; Nino, D.; Murcar-Evans, B. I.; Milstein, J. N.; Kraskouskaya, D.; Gunning, P. T. Sensitive detection of broad-spectrum bacteria with small-molecule fluorescent excimer chemosensors. *ACS Sens.* **2020**, *5*, 2753–2762.

(21) Jung, H. S.; Park, M.; Han, D. Y.; Kim, E.; Lee, C.; Ham, S.; Kim, J. S. Cu²⁺ ion-induced self-assembly of pyrenylquinoline with a pyrenyl Excimer Formation. *Org. Lett.* **2009**, *11*, 3378–3381.

(22) Zeng, L.; Wu, J.; Dai, Q.; Liu, W.; Wang, P.; Lee, C. Sensing of bacterial endotoxin in aqueous solution by supramolecular assembly of pyrene derivative. *Org. Lett.* **2010**, *12*, 4014–4017.

(23) Wilkins, R. G. *Kinetics and mechanisms of reactions of transition metal complexes*, 2nd ed.; VCH: New York, 1991.

- (24) Kim, J.; Oh, J.; Han, M. S. A ratiometric fluorescence probe for the selective detection of H₂S in serum using a pyrene-DPA-Cd²⁺ complex. *RSC Adv.* **2021**, *11*, 24410–24415.
- (25) Li, H.; Yang, T.; Liao, T.; Debowski, A. W.; Nilsson, H.; Fulurija, A.; Haslam, S. M.; Mulloy, B.; Dell, A.; Stubbs, K. A.; Marshall, B. J.; Benghezal, M. The redefinition of *Helicobacter pylori* lipopolysaccharide O-antigen and core-oligosaccharide domains. *PLoS Pathog.* **2017**, *13*, No. e1006280.
- (26) Wen, L.; Lv, J.; Chen, L.; Li, S.; Mou, X.; Xu, Y. A fluorescent probe composed of quantum dot labeled aptamer and graphene oxide for the determination of the lipopolysaccharide endotoxin. *Microchim. Acta* **2019**, *186*, 122.
- (27) Zhang, Z.; Yang, J.; Pang, W.; Yan, G. An aptamer-based fluorescence probe for facile detection of lipopolysaccharide in drinks. *RSC Adv.* **2017**, *7*, 54920–54926.
- (28) Gao, J.; Lai, Y.; Wu, C.; Zhao, Y. Exploring and exploiting the synergy of non-covalent interactions on the surface of gold nanoparticles for fluorescent turn-on sensing of bacterial lipopolysaccharide. *Nanoscale* **2013**, *5*, 8242–8248.
- (29) Gao, J.; Li, Z.; Zhang, O.; Wu, C.; Zhao, Y. Tunable accessibility of dye-doped liposomes towards gold nanoparticles for fluorescence sensing of lipopolysaccharide. *Analyst* **2017**, *142*, 1084–1090.
- (30) Zhu, Y.; Xu, C.; Wang, Y.; Chen, Y.; Ding, X.; Yu, B. Luminescent detection of the lipopolysaccharide endotoxin and rapid discrimination of bacterial pathogens using cationic platinum(II) complexes. *RSC Adv.* **2017**, *7*, 32632–32636.
- (31) Lan, M.; Wu, J.; Liu, W.; Zhang, W.; Ge, J.; Zhang, H.; Sun, J.; Zhao, W.; Wang, P. Copolythiophene-derived colorimetric and fluorometric sensor for visually supersensitive determination of lipopolysaccharide. *J. Am. Chem. Soc.* **2012**, *134*, 6685–6694.
- (32) Wu, J.; Zawistowski, A.; Ehrmann, M.; Yi, T.; Schmuck, C. Peptide functionalized polydiacetylene liposomes act as a fluorescent turn-on sensor for bacterial lipopolysaccharide. *J. Am. Chem. Soc.* **2011**, *133*, 9720–9723.
- (33) Jiang, G.; Wang, J.; Yang, Y.; Zhang, G.; Liu, Y.; Lin, H.; Zhang, G.; Li, Y.; Fan, X. Fluorescent turn-on sensing of bacterial lipopolysaccharide in artificial urine sample with sensitivity down to nanomolar by tetraphenylethylene based aggregation induced emission molecule. *Biosens. Bioelectron.* **2016**, *85*, 62–67.
- (34) Huang, L.; Tao, H.; Zhao, S.; Yang, K.; Cao, Q.; Lan, M. A tetraphenylethylene-based aggregation-induced emission probe for fluorescence turn-on detection of lipopolysaccharide in injectable water with sensitivity down to picomolar. *Ind. Eng. Chem. Res.* **2020**, *59*, 8252–8258.
- (35) Tang, Y.; Kang, A.; Yang, X.; Hu, L.; Tang, Y.; Li, S.; Xie, Y.; Miao, Q.; Pan, Y.; Zhu, D. A robust OFF-ON fluorescent biosensor for detection and clearance of bacterial endotoxin by specific peptide based aggregation induced emission. *Sens. Actuators, B* **2020**, *304*, No. 127300.
- (36) Khownum, K.; Romsaiyud, J.; Borwornpinyo, S.; Wongkrasant, P.; Pongkorpakol, P.; Muanprasat, C.; Boekfa, B.; Vilaivan, T.; Ruchirawat, S.; Limtrakul, J. Turn-on fluorescent sensor for the detection of lipopolysaccharides based on a novel bispyrenyl terephthalaldehyde-bis-guanyldiazone. *New J. Chem.* **2019**, *43*, 7051–7056.
- (37) Jones, G.; Jiang, H. Detection of lipopolysaccharide and lipid A employing a spermine-pyrene conjugate. *Bioconjugate Chem.* **2005**, *16*, 621–625.
- (38) Kalyanasundaram, K.; Thomas, J. K. Environmental effects on vibronic band intensities in pyrene monomer fluorescence and their application in studies of micellar systems. *J. Am. Chem. Soc.* **1977**, *99*, 2039–2044.
- (39) Dong, D. C.; Winnik, M. A. The Py scale of solvent polarities. *Can. J. Chem.* **1984**, *62*, 2560–2565.
- (40) Bains, G.; Patel, A. B.; Narayanaswami, V. Pyrene: a probe to study protein conformation and conformational changes. *Molecules* **2011**, *16*, 7909–7935.
- (41) Bergstrand, A.; Svanberg, C.; Langton, M.; Nydén, M. Aggregation behavior and size of lipopolysaccharide from *Escherichia coli* O55:B5. *Colloids Surf., B* **2006**, *53*, 9–14.
- (42) Redeker, C.; Briscoe, W. H. Interactions between mutant bacterial lipopolysaccharide (LPS-Ra) Surface Layers: surface vesicles, membrane fusion, and effect of Ca²⁺ and temperature. *Langmuir* **2019**, *35*, 15739–15750.
- (43) Schwarz, H.; Gornicec, J.; Neuper, T.; Parigiani, M. A.; Wallner, M.; Duschl, A.; Horejs-Hoeck, J. Biological activity of masked endotoxin. *Sci. Rep.* **2017**, *7*, 44750.
- (44) Hardy, E.; Kamphuis, T.; Japaridze, A.; Wilschut, J. C.; Winterhalter, M. Nanoaggregates of micropurified lipopolysaccharide identified using dynamic light scattering, zeta potential measurement, and TLR4 signaling activity. *Anal. Biochem.* **2012**, *430*, 203–213.
- (45) Sali, W.; Patoli, D.; Pais De Barros, J.; Labbé, J.; Deckert, V.; Duhéron, V.; Le Guern, N.; Blache, D.; Chaumont, D.; Lesniewska, E.; Gasquet, B.; Paul, C.; Moreau, M.; Denat, F.; Masson, D.; Lagrost, L.; Gautier, T. Polysaccharide chain Length of lipopolysaccharides from *Salmonella* Minnesota is a determinant of aggregate stability, plasma residence time and proinflammatory propensity *in vivo*. *Front. Microbiol.* **2019**, *10*, 1774.
- (46) Andrä, J.; Koch, M. H. J.; Bartels, R.; Brandenburg, K. Biophysical characterization of endotoxin inactivation by NK-2, an antimicrobial peptide derived from mammalian NK-lysin. *Antimicrob. Agents Chemother.* **2004**, *48*, 1593–1599.
- (47) Sun, J.; Ge, J.; Liu, W.; Wang, X.; Fan, Z.; Zhao, W.; Zhang, H.; Wang, P.; Lee, S. A facile assay for direct colorimetric visualization of lipopolysaccharides at low nanomolar level. *Nano Res.* **2012**, *5*, 486–493.
- (48) Kennedy, S.; Caddy, B.; Douse, J. M. F. Micellar electrokinetic capillary chromatography of high explosives utilising indirect fluorescence detection. *J. Chromatogr. A* **1996**, *726*, 211–222.
- (49) Li, W.; Zhou, H.; Nawaz, M. A. H.; Niu, N.; Yang, N.; Ren, J.; Yu, C. A perylene monoimide probe based fluorescent micelle sensor for the selective and sensitive detection of picric acid. *Anal. Methods* **2020**, *12*, 5353–5359.
- (50) Cho, H. K.; Lee, D. H.; Hong, J. A fluorescent pyrophosphate sensor via excimer formation in water. *Chem. Commun.* **2005**, *13*, 1690–1692.